Dynamic modelling and part-load behavior of a Brayton heat pump

Matteo Pettinari [a,*], Guido Francesco Frate [a], Konstantinos Kyprianidis [b], Lorenzo Ferrari [a]

[a] *University of Pisa, Department of Energy, Systems, Territory and Construction Engineering, Pisa, Italy*

[b] *Mälardalen University, Department of Sustainable Energy Systems, School of Business, Society and Engineering, Västerås, Sweden*

**corresponding author*: matteo.pettinari@phd.unipi.it

Abstract

Among the environmentally friendly technologies recently proposed in the literature, high-temperature heat pumps represent a promising solution to foster the complete penetration of renewables within the power grid. Such systems may be based on closed Brayton cycles and leverage many existing components. As they are meant to provide high-temperature heat while using renewable electricity, their potential field of application ranges from industrial heating to energy storage. Several variants are currently under development to assess the feasibility of such systems in providing flexibility to the electricity grid. To do so, they need to operate in part-load conditions and quickly react when the load must be adjusted. In this regard, this study investigates the transient capabilities of Brayton heat pump technology. To this extent, a detailed transient model of a novel prototype proposed in the literature is presented, accounting for controls, thermal inertia and volume dynamics related to heat exchangers and piping. Furthermore, the model is used to assess the transient performance of the system in response to sudden load variations, which is achieved by adapting the turbomachinery operating velocities. Results show that the system can safely operate in part-load conditions with regulation times compatible with industrial needs.

Keywords: high-temperature heat pump; dynamic modelling; transient simulation; control system.

Nomenclature

Abbreviations:

NTU	number of transfer unit, −
SM	surge margin, −
PR	pressure ratio, −
OV	overshoot, %
COP	coefficient of performance, −

Letter symbols:

t	time, s
$\dot{m}$	mass flow rate, kg/s
p	pressure, Pa
T	temperature, K
$\dot{T}$	temperature slope, K/min
ΔT	temperature difference, K
N	rotational speed, rpm
$\dot{Q}$	heat transfer rate, W
C	heat capacity rate, W/K

Greek symbols:

ε	effectiveness, −
τ	torque, N m

Subscripts and superscript:

0	reference state
1,2,3,..	cycle points
$corr$	corrected
r	ratio
min	minimum
max	maximum
hot	hot fluid/side
$cold$	cold fluid/side
$tube$	tube side
$shell$	shell side
$wall$	wall
$overall$	overall
$surge$	surge conditions
op	operating conditions
$rise$	rise
$settl$	settling

1. Introduction

According to the latest International Energy Agency report [1], heat production constitutes the world's largest energy end use, accounting for almost half of the global final energy consumption. Of the energy consumed for heat production in 2021, industry accounted for nearly 51 %, whilst 46 % was consumed for domestic purposes, such as

space and water heating in buildings, and 3 % in agriculture-related activities. Since fossil fuels still cover over 60 % of heating energy demand [1], heat production decarbonization represents a vital step towards carbon neutrality.

Among the solutions to decrease carbon dioxide emission due to heating, high-temperature heat pumps are increasingly recognized as a key technology [2]. Because of the progressive penetration of renewable energy sources, heat pumps may leverage excess renewable energy to recover heat from low-temperature sources (e.g., ambient heat, waste heat sources) and supply it to high-temperature heat utilizers (e.g. industrial processes or thermal energy storage), thus securing sustainable heating. Various heat pumps are available in the market, namely vapour compression, absorption, rotation, hybrid, and transcritical heat pumps [3]. The most common ones operate according to the Rankine thermodynamic cycle, although other cycles, such as Brayton heat pumps, were found to provide advantages depending on the process' source and sink temperature profile under consideration [4].

Arpagaus et al. [5] reported that most commercially available industrial heat pumps provide heat up to 90 °C, whilst only a few plants can supply heat at temperatures in the 140−160 °C range. Apart from domestic purposes, current fields of application comprise food, pulp and paper, metal, and chemical industries, as they benefit from low-temperature heat. Furthermore, several studies have shown a large demand for high-temperature heat in the European industry [6,7]. Therefore, such systems' range of utilization would likely extend in case higher heat temperatures were reached. For instance, heat pumps could serve for low-pressure steam production [5].

Low efficiencies, high equipment cost, long payback periods, component limitations, and the lack of environmentally friendly operating fluids performing adequately at high temperatures represent the main limitations to heat pump development [8]. However, Zühlsdorf et al. [9] suggest that heat pumps capable of supplying heat to at least 280 °C can be technically and economically feasible, for instance, by adopting equipment available in the oil and gas industry. Several concepts capable of delivering heat above 150 °C have been proposed in the literature for industrial purposes [5]. Further prototypes have also been proposed for energy storage applications [10]. Nevertheless, these heat pumps must be developed, built, and integrated into the relevant industries. Besides, such systems should also bring flexibility to the power grid, allowing for quick start-ups and load variations whilst operating safely and ideally at high efficiencies.

Despite being crucial for the demonstration of such technology, only a few works have so far focused on the transient capabilities of Brayton heat pumps. In particular, Frate et al. [11] investigated the power regulation of a Brayton PTES system through fluid inventory control, whilst other works analysed the behaviour of such systems during cold start-up [12,13]. As a contribution to this research topic, the paper investigates the transient capabilities of a novel Brayton heat pump. Particular focus is set on its response to sudden variations in the desired heat sink temperature by regulating the turbo-compressor operating speed.

2. Case study

The Brayton heat pump concept recently proposed by the German Aerospace Center (DLR) [12,14] and currently under realization in Cottbus, Germany, was considered in the present work. As a novel prototype, the heat pump aims to deliver heat at more than 250 °C. Figure 1 reports the plant layout, mainly comprising a three-stage turbo-compressor, three shell-and-tube heat exchangers, and a two-stage axial turbine.

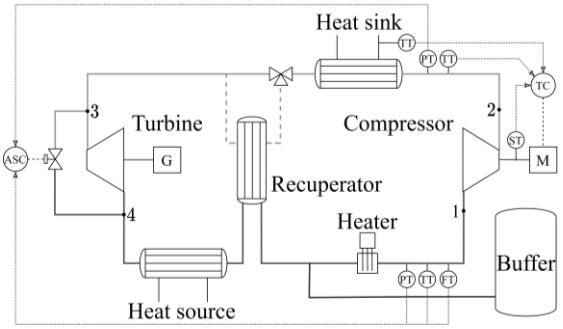

Figure 1: High-temperature heat pump layout.

The system operates according to the Brayton cycle. At first, the compressor increases a given operating fluid (e.g., dry air, Argon, or CO_2) temperature and pressure (pt. 1-2) whilst using electric power. The useful heat is then transferred to the thermal user employing the high-temperature heat exchanger (pt. 2-3), and afterwards, the fluid is expanded through the turbine to recover power and resultingly cool the fluid down to sub-ambient temperatures (pt. 3-4). A further heat exchanger transfers heat to the fluid from a low-temperature heat source (e.g., the environment) before returning it to the compressor (pt. 4-1). Moreover, a recuperator can recover heat internally, while a heater can also provide additional heat to raise the gas temperature at the compressor inlet. In the present work, the recuperator is assumed to be disabled, although present in the actual plant layout. In such a setup, the system supplies heat for 115 kW at 272 °C with a coefficient of performance (COP) of around 1.3. Finally, the system operates as a closed cycle, enabling fluid

inventory control to adjust the provided thermal load by extracting/injecting mass into the system from a secondary circuit (schematized as a buffer for simplicity). However, such a control strategy is not analysed in the present work.

3. Methodology

The heat pump was modelled within the Simulink® environment of Matlab® R2022b [15]. The Simscape™ package was used as it allows for easily implementing control systems due to the integration with Simulink®. For what concerns the operating fluids, dry air was considered in the closed cycle and secondary processes. It was modelled as a real gas, and its thermophysical properties were computed through RefProp [16].

3.1. Turbomachinery

The compressor and turbine were modelled at a system level and assumed adiabatic with negligible gas volume. The turbomachinery thermal dynamics were neglected, while rotor dynamics were considered by accounting for the compressor, turbine, motor, generator, and transmission moments of inertia.

As for the turbomachines' off-design modelling, actual performance maps provided by DLR were used, thereby specifying the relation between the conditions at the machine inlet (e.g., mass flow rate, pressure and temperature) with the component pressure ratio and the adiabatic efficiency. Figure 2 reports the compressor map used in the present work.

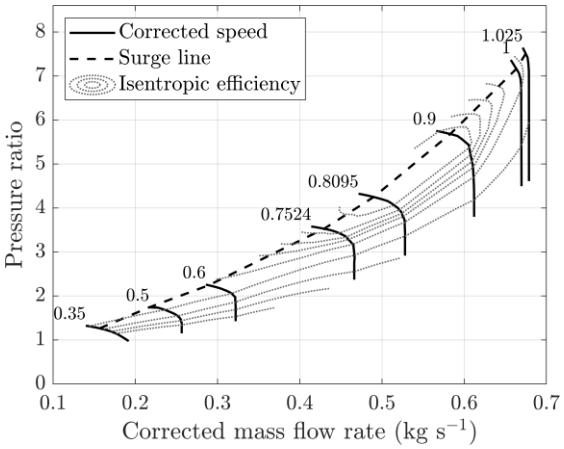

Figure 2: Compressor performance map [12].

It is worth noting that corrected parameters, defined as in Eq. (1), were used to account for pressure and temperature variations at the machine inlet:

$$\begin{cases} \dot{m}_{corr} = \dot{m}\dfrac{\sqrt{T/T_0}}{p/p_0} \\ N_{corr} = \dfrac{N}{\sqrt{T/T_0}} \end{cases} \quad (1)$$

where $p_0 = 101325$ Pa, $T_0 = 288.15$ K, N is the rotational speed, and $\dot{m}$, T, p are the inlet mass flow, temperature, and pressure, respectively.

3.2. Heat Exchangers

Similarly to the turbomachinery, the three shell-and-tube heat exchangers were assumed adiabatic and modelled based on the technical data provided by the manufacturer [12]. Therefore, characteristics such as geometry, flow arrangement, and metal mass were used to customize the components available in the Simscape™ Fluids library [17]. From a general standpoint, the flow conditions at each side of the heat exchangers were determined by means of mass, momentum, and energy balances. Conversely, the heat transfer rate exchanged between the two sides was established according to the ε-NTU methodology [18] as in Eq. (2):

$$\begin{cases} \dot{Q} = \varepsilon \cdot C_{min} \cdot \left(T_{hot,in} - T_{cold,in}\right) \\ NTU = \dfrac{1}{C_{min} R_{overall}} \\ \varepsilon = f(NTU, C_r) \end{cases} \quad (2)$$

where $\dot{Q}$ is the heat flow rate through the heat exchanger, ε is the heat exchanger effectiveness depending on the flow arrangement, C_{min} is the minimum heat capacity rate between the hot and cold side, C_r is the ratio between minimum and maximum heat capacity rate, and $R_{overall}$ is the overall thermal resistance of the heat exchangers.

Thermal inertia effects were further considered by modelling the thermal capacity due to the metal mass of the heat exchanger. The heat transfer rate at each side of the exchanger was then computed as:

$$\dot{Q}_{tube} = \dot{Q} + C_{wall,tube}\dot{T}_{wall,tube} \quad (3)$$

$$\dot{Q}_{shell} = \dot{Q} - C_{wall,shell}\dot{T}_{wall,shell} \quad (4)$$

where $C_{wall,i}$ is the thermal capacity of the heat exchangers evenly divided between the tube and shell sides, $\dot{T}_{wall,i}$ is the temperature slope in the wall half (positive if the temperature increases, negative when it drops), and $\dot{Q}$ is the heat transfer rate computed according to Eq. (2).

3.3. Piping, valves, and ancillary equipment

Piping's contribution to the system gas volume and its thermal inertia was accounted for in the model. In particular, pipes were assumed adiabatic, and their volumes and metal mass were determined based on their actual geometry. Similarly, the turbine bypass and recuperation valves were modelled as adiabatic local restrictions with negligible volume. Their geometry, as well as their flow characteristic, were specified based on

manufacturer data. Finally, only pressure drops were considered for what concerns the heater.

3.4. Control strategy

Two control loops were designed to safely operate the system in transient conditions, namely:

- anti-surge controller;
- temperature controller.

The former prevented the compressor from operating within critical areas near the surge line. In more detail, the compressor surge was avoided by varying the turbine bypass opening to increase the compressor flow, as shown in Figure 1. Moreover, the valve opening was determined by a variable-gain PI feedback controller based on the surge margin residual. In the present work, a minimum surge margin of 10 % was ensured through the anti-surge regulator and computed as:

$$SM = \left(\frac{PR_{surge}}{PR_{op}} - 1 \right)_{\dot{m}_{corr}} \quad (5)$$

where PR_{op} is the operating pressure ratio, whilst PR_{surge} is the surge line pressure ratio evaluated at the same corrected mass flow.

On the other hand, the temperature controller was used to regulate the sink outlet temperature at the desired setpoint by properly varying the motor/compressor speed. As the purpose of the analysis was to investigate the system response and not to optimize the system performance, only the following control requirements were considered:

- zero steady-state residual due to variations in the sink outlet temperature setpoint;
- temperature slopes of no more than 2 K/min to avoid critical thermal stresses at the heat exchangers [12].

A cascade architecture was considered to meet the considered requirements. Figure 3 reports the control schematic.

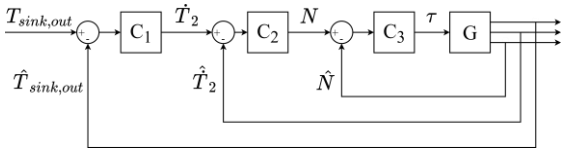

Figure 3: Temperature control schematic.

Three control loops were implemented, each one characterized by a time-continuous PI regulator. The outer loop was used to determine a setpoint for the compressor outlet temperature slope based on the sink outlet temperature residual. Here, the slope setpoint was limited to a maximum value of ± 2 K/min to avoid undesired stresses at the high-temperature heat exchanger. The intermediate control loop then compares the temperature slope setpoint with its measurement (or estimate), thus providing a motor speed setpoint. In analogy to the outer loop, the speed setpoint was limited to guarantee the compressor rotates at admissible shaft speeds. Lastly, the inner controller determined the motor torque based on the speed error. In this regard, the motor speed ramp limits were not accounted for within the control architecture for simplicity. However, the resulting shaft accelerations were verified a posteriori to ensure they did not exceed the maximum limit of 300 rpm/s. Finally, anti-windup methods were adopted to prevent integration wind-up of the regulators.

4. Results and Discussion

4.1. Performed analyses

The heat pump model presented in the previous sections was used to study the system behaviour in response to sudden variations of the sink outlet temperature demand.

A sink outlet temperature increment of 10 °C was considered at first to investigate the system's response in detail. Such a simulation aims at assessing the characteristic response time of the system and the main issues that occur when the high-temperature secondary process requires a given mass flow but at a higher temperature with respect to the nominal one. Secondly, a sensitivity analysis was performed by varying the sink outlet temperature setpoint of up to 20 °C. Here, the primary purpose was to explore the operability range of the system when driven by such a regulation approach. Finally, a further analysis was performed to assess the impact of the maximum allowed thermal stresses at the heat exchangers on the system response by simulating the system for the same required sink outlet temperature lift and different discharge temperature slope limits of the compressor.

At the beginning of each scenario, the system was assumed to operate at nominal, steady conditions, delivering heat for 115 kW at 272 °C to the secondary process, raising its fluid temperature to 261.4 °C. Therefore, all the components were assumed already in steady-state temperature, and turbomachines rotating at their nominal speeds. Finally, it is worth mentioning that control actuators such as the heater and the recuperation three-way valve were not utilised in the present analyses, despite being accounted for in the model. In particular, the three-way valve was regulated such that the primary mass flow exiting the high-temperature heat exchanger went directly to the turbine inlet.

4.2. Setpoint variation

The system response due to a step change in the sink outlet temperature demand is shown in Figure 4. At the beginning of the simulation, the

system operates at nominal conditions, heating the sink flow from 15 °C to around 261 °C. At t = 5 min, the desired temperature at the sink outlet is suddenly increased by 10 °C. As reported in Figure 4b, to accommodate the setpoint movement, the temperature controller accelerates the compressor, which provides a higher and hotter mass flow rate at the high-temperature heat exchanger. As the primary flow and its temperature increase, more heat is transferred to the secondary process, and the sink mass flow outer temperature rises to the desired value.

From a transient perspective, the sink outlet temperature evolves as a second-order response characterized by a settling time of 12.5 min and an overshoot of 9.5 %. Moreover, during the rise time (t_{rise} = 6.45 min), it can be observed that the sink outlet temperature increases almost constantly due to the temperature controller. As reported in Figure 4b, to prevent thermal stresses at the heat exchanger, the controller accelerates the compressor while ensuring its outer temperature (e.g. T_2) does not rise with slopes higher than 2 K/min. In particular, both the relative speed and the sink outlet temperature vary linearly when the maximum allowed slope is reached. As the temperature slope limit bounds the machine acceleration, it can be stated that it represents a critical parameter characterizing the system response to sudden temperature variations. Allowing for higher slopes by adopting more advanced heat exchangers may likely shorten the rise time.

On the other hand, nearly before t = 15 min, the measured sink outlet temperature experiences some oscillations, which extend the response time to around 3−4 min. Here, both overshoots and undershoots are primarily due to the thermal inertia of the heat exchangers and piping. When optimizing the system response, adopting more sophisticated regulators with a feedforward component (e.g., FF-FB or MPC) may be considered to dampen the oscillations, thus further shortening the response time. From t = 20 min until the end of the simulation, the compressor speed is slowly adjusted as the temperatures within the heat exchangers and piping settle.

It is also interesting to observe how the system performance varies during the simulation. Figure 4c reports the plant COP and the main quantities involved in its calculation. It can be observed that the COP decreases from around 1.30 to 1.18 during the regulation and finally settles to 1.27 as the new operating conditions are met. This is strictly related to the control strategy under analysis that varies the compressor operating point. Since the compressor rotates at higher speeds, it operates at lower efficiencies, absorbing more power. Although the exchanged thermal power and

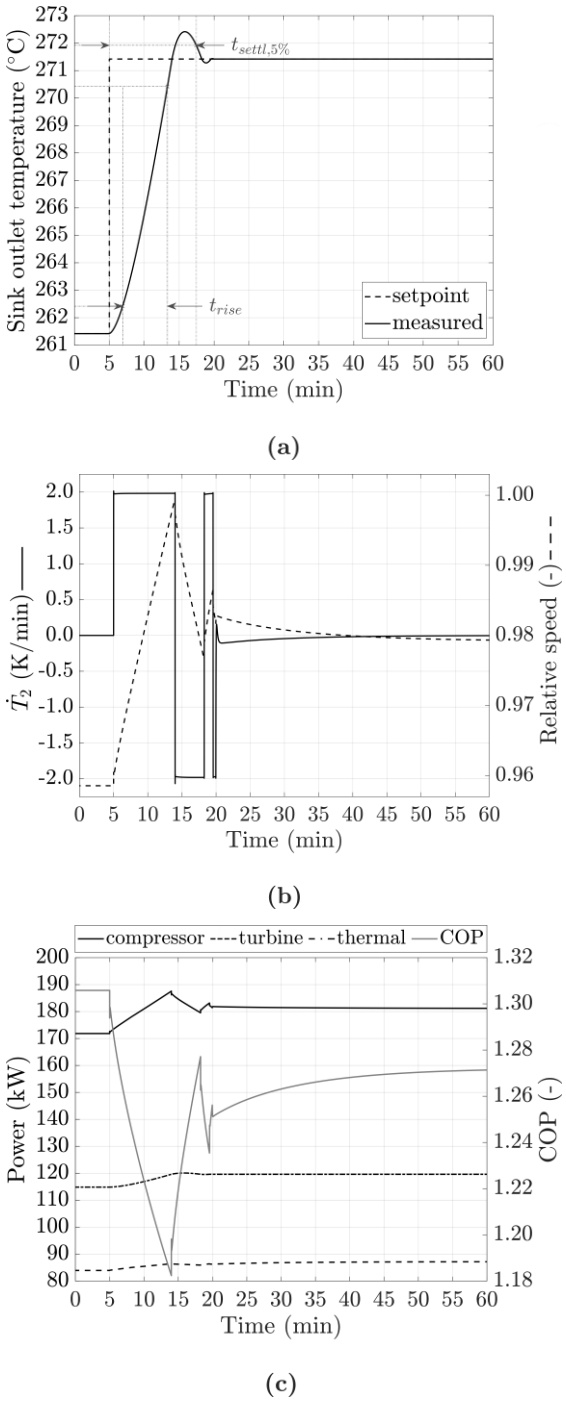

Figure 4: System response to a variation of the desired sink outlet temperature: (a) sink outlet temperature; (b) control signals; (c) system performance.

the power recovered by the turbine also increase due to the higher and hotter mass flow rate circulating within the closed cycle, they vary less significantly than in the compressor. Therefore, the overall system COP is lower. Finally, it is worth noting the differences among the compressor, turbine, and thermal power exchanged through the high-pressure heat exchanger during the regulation of the system (t = 5–20 min). In particular, the heat exchanger's thermal inertia helps mitigate the

abrupt variations of the power absorbed by the compressor, resulting in smoother profiles for both the exchanged thermal power and the power recovered by the turbine.

4.3. Sensitivity to the desired sink temperature lift

A sensitivity analysis was performed to compare the system behaviour for different temperature setpoint variations and to investigate the adopted control strategy's limit. Results are shown in Figure 5, which reports the sink outlet temperature, the measured temperature slope at the compressor outlet and the motor/compressor relative speed. Table 1 summarizes the main properties characterizing the sink outlet temperature responses instead.

Table 1: Sink outlet temperature response characteristics for different desired temperature steps.

ΔT (°C)	t_{rise} (min)	$t_{settl,5\%}$ (min)	OV (%)
-20	10.95	18.73	6.47
-15	8.75	15.82	7.82
-10	6.47	12.52	9.88
-5	3.93	8.5	14
5	3.93	8.5	13.92
10	6.45	12.5	9.97
15	9.91	13.53	0.41
20	25.8	40.85	-

In each considered scenario, it can be observed that both the compressor speed and the sink outlet temperature constantly increase as the setpoint perturbations occur due to temperature control. As discussed in the previous section, the rate at which these quantities rise depends on the maximum thermal stress sustainable by the heat exchangers. Furthermore, except for temperature increments of 15−20 °C, each response oscillates and stabilizes at the desired value.

It can be noted that the system response is symmetrical with respect to the nominal conditions. As reported in Table 1, in the case of changes of equal magnitude, the system exhibits almost identical response times to reach the new operating conditions. The oscillation magnitude is also similar, although it is the sign of the variation to determine whether the sink outlet temperature undergoes an overshoot or an undershoot. Different behaviour is observed in the case of increments higher than ten degrees. For a required temperature step of 15 °C, the sink outlet temperature does not experience any overshoot and shows a longer rise time and shorter settling time compared to a temperature variation of −15 °C. On the other hand, the system takes more than 40 min to increase the sink outlet temperature of 20 °C, and zero steady error is reached slightly after one hour.

These differences are related to how faster the compressor can operate compared to the nominal

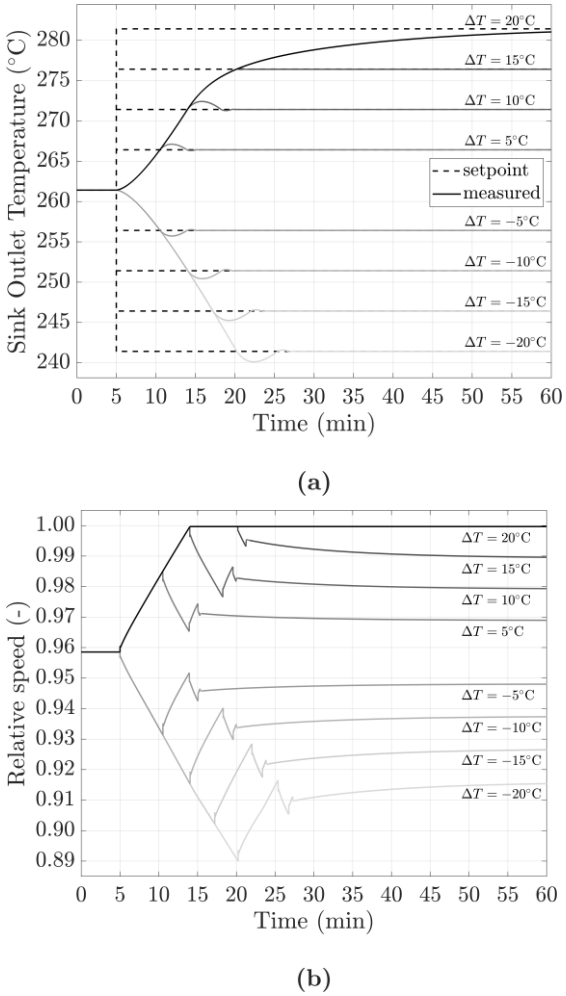

Figure 5: Sensitivity to the temperature setpoint variation: (a) measured sink outlet temperature; (b) relative motor/compressor speed.

operating point, which primarily depends on its performance map. As reported in Figure 5b, in such cases, the relative speed of the motor/compressor continuously increases until it reaches the maximum limit of 1, meaning that the compressor is operating at its maximum speed and cannot increase its outlet temperature any further. Consequently, since the compressor cannot provide higher and hotter mass flow at the heat exchanger, more time is required for the heat exchanger material to warm up and overcome its thermal inertia, eventually leading to a rise in the sink outlet temperature. Such behaviour also implies that higher sink outlet temperature step increments are not achievable by the system through the proposed regulation strategy.

Conversely, such issues do not occur in the case of a desired temperature reduction at the sink outlet as the compressor decelerates to reduce the heat transferred through the high-temperature heat exchanger, thus decreasing the sink outlet temperature. Here, depending on the temperature step magnitude (e.g., ΔT = −15,−20 °C), it is worth

pointing out that the anti-surge regulator may be enabled to avoid compressor surge, thus ensuring the system operates safely.

4.4. Sensitivity to the maximum temperature slope

The system response to a desired sink outlet temperature step of 10 °C is reported in Figure 6. Different maximum compressor outlet temperature slopes are considered, which results in higher thermal stresses at the heat exchangers being allowed.

As shown in Figure 6a and Table 2, higher slopes lead to quicker response times. In particular, both the rise and settling times reduce significantly when a temperature slope of 5 K/min is permitted. Further improvements are achieved for slopes of 10−15 K/min, although less relevant (e.g., the settling time difference is around 1 min when comparing results obtained using slopes of 5 K/min and 10 K/min, whilst less than 20 s for slopes of 10 K/min and 15 K/min). The transients' quality also improves when higher thermal stresses are allowed, as the response maximum overshoot reduces by one-half for 5 K/min slopes and becomes negligible for 10−15 K/min.

Table 2: Sink outlet temperature response characteristics for different allowed temperature slopes at the compressor outlet.

$\dot{T}_{2,max}$ (K/min)	t_{rise} (min)	$t_{settl,5\%}$ (min)	OV (%)
2	6.45	12.5	9.97
5	3.68	5.06	4.01
10	3.08	4.13	1.25
15	2.98	3.82	0.51

From a general standpoint, the higher slopes lead to quicker responses as they permit steeper speed ramps, as reported in Figure 6b. As a result, the compressor can provide higher mass flow at the maximum reachable temperature sooner at the high-temperature heat exchanger, thus shortening the time required to raise the sink outlet temperature. The same also holds for the response oscillations, which become lower and lower as higher temperature slopes at the compressor outlet are considered. However, despite allowing for quicker responses, almost negligible improvements are observed when increasing the maximum slope from 10 K/min to 15 K/min, which suggests that using heat exchangers capable of sustaining higher thermal gradients may not be practical, as they would likely be more complex and expensive whilst providing similar performance.

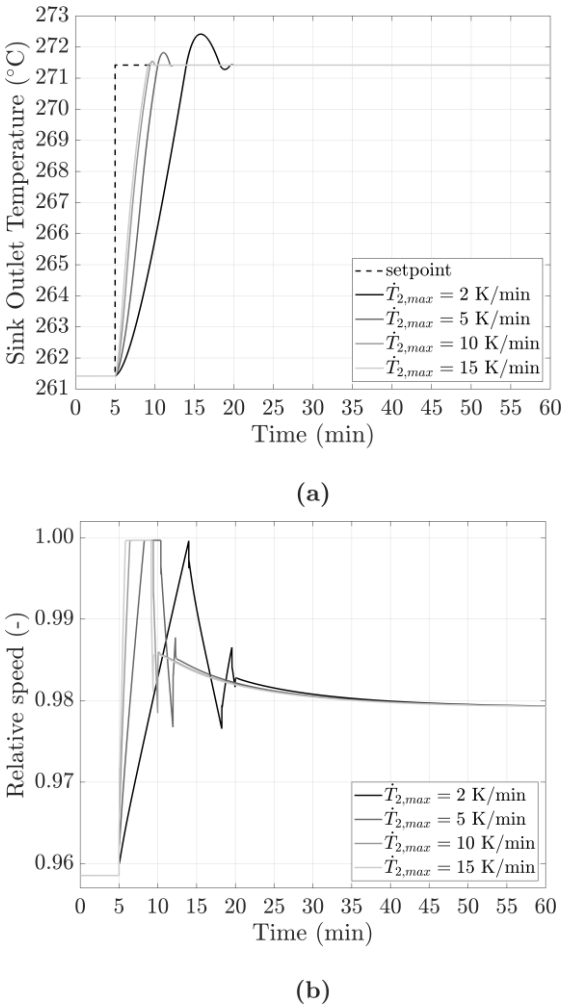

Figure 6: Sensitivity to the compressor outlet maximum allowed temperature slope: (a) measured sink outlet temperature; (b) relative motor/compressor speed.

5. Conclusions

The paper analyzed the transient behaviour of a Brayton heat pump responding to a desired temperature variation at the sink outlet by varying the compressor operating speed. To this extent, a detailed system model was developed, and control loops were designed to safely operate the system in transient conditions. The model was then used to investigate the system response for a required sink outlet temperature increment and to analyze the range of applications of the considered control strategy. Results can be summarized in the following statements:

- the system raises the sink outlet temperature to the desired value with a second-order system response. The response is symmetrical with respect to the nominal operating conditions;
- the rate at which the sink outlet temperature increases is limited by the maximum allowed temperature slope at the compressor outlet. Heat exchangers capable of sustaining higher thermal stresses are then required to reduce the system response time;
- oscillations characterizing the system response are primarily due to the system's thermal inertia. More sophisticated controllers may be

considered to avoid overshoots, further improving the system transient;
- the maximum sink outlet temperature achievable by the heat pump is limited by the maximum operating speed of the compressor, which also affects the system response time for desired temperature lifts higher than 10 °C.
- allowing for higher thermal stresses at the heat exchangers leads to faster system responses, although the improvements progressively decrease for temperature slopes higher than 5 K/min.

Acknowledgment

The authors would like to acknowledge Johannes Oehler, Anh Phong Tran, and Panagiotis Stathopoulos from DLR for providing detailed data concerning the Brayton heat pump under analysis and for their support and feedback.

This research has received financial contribution from the Italian Operative National Plan (Piano Operativo Nazionale, PON) in the framework of the project Ricerca e Innovazione 2014−2020 (PON R&I) – Azioni IV.4 e IV.5 “Dottorati di ricerca su tematiche dell'innovazione e green” (DM MUR 1061/2022) e IV.6 “Contratti di ricerca su tematiche dell'innovazione e green” (DM MUR 1062/2022).

References

[1] IEA, 2022, *Heating*, IEA, Paris, https://www.iea.org/reports/heating (last accessed: 30/05/2023)

[2] IEA, 2022, *The Future of Heat Pumps*, IEA, Paris, https://www.iea.org/reports/the-future-of-heat-pumps (last accessed: 30/05/2023).

[3] Wolf, S., and Blesl, M., 2016, “Model-Based Quantification of the Contribution of Industrial Heat Pumps to the European Climate Change Mitigation Strategy,” *ECEEE Industrial Summer Study Proceedings*, Berlin, Germany, pp. 477–487.

[4] Gai, L., Varbanov, P. S., Walmsley, T. G., and Klemeš, J. J., 2020, “Critical Analysis of Process Integration Options for Joule-Cycle and Conventional Heat Pumps,” Energies, **13**(3), p. 635. https://doi.org/10.3390/en13030635.

[5] Arpagaus, C., Bless, F., Uhlmann, M., Schiffmann, J., and Bertsch, S. S., 2018, “High Temperature Heat Pumps: Market Overview, State of the Art, Research Status, Refrigerants, and Application Potentials,” Energy, **152**, pp. 985–1010. https://doi.org/10.1016/j.energy.2018.03.166.

[6] Naegler, T., Simon, S., Klein, M., and Gils, H. C., 2015, “Quantification of the European Industrial Heat Demand by Branch and Temperature Level: Quantification of European Industrial Heat Demand,” Int. J. Energy Res., **39**(15), pp. 2019–2030. https://doi.org/10.1002/er.3436.

[7] Rehfeldt, M., Fleiter, T., and Toro, F., 2018, “A Bottom-up Estimation of the Heating and Cooling Demand in European Industry,” Energy Effic., **11**(5), pp. 1057–1082. https://doi.org/10.1007/s12053-017-9571-y.

[8] Jesper, M., Schlosser, F., Pag, F., Walmsley, T. G., Schmitt, B., and Vajen, K., 2021, “Large-Scale Heat Pumps: Uptake and Performance Modelling of Market-Available Devices,” Renew. Sustain. Energy Rev., **137**, p. 110646. https://doi.org/10.1016/j.rser.2020.110646.

[9] Zühlsdorf, B., Bühler, F., Bantle, M., and Elmegaard, B., 2019, “Analysis of Technologies and Potentials for Heat Pump-Based Process Heat Supply above 150 °C,” Energy Convers. Manag. X, **2**, p. 100011. https://doi.org/10.1016/j.ecmx.2019.100011.

[10] Smith, N. R., Tom, B., Rimpel, A., Just, J., Marshall, M., Khawly, G., Revak, T., and Hoopes, K., 2022, “The Design of a Small-Scale Pumped Heat Energy Storage System for the Demonstration of Controls and Operability,” *Proceedings of the ASME Turbo Expo 2022: Turbomachinery Technical Conference and Exposition*. *Volume 4: Cycle Innovations; Cycle Innovations: Energy Storage*. Rotterdam, Netherlands. V004T07A012. ASME. https://doi.org/10.1115/GT2022-83424

[11] Frate, G. F., Pettinari, M., Di Pino Incognito, E., Costanzi, R., and Ferrari, L., 2022, “Dynamic Modelling of a Brayton PTES System,” *Proceedings of the ASME Turbo Expo 2022: Turbomachinery Technical Conference and Exposition*. *Volume 4: Cycle Innovations; Cycle Innovations: Energy Storage*. Rotterdam, Netherlands. V004T07A013. ASME. https://doi.org/10.1115/GT2022-83445.

[12] Oehler, J., Tran, A. P., and Stathopoulos, P., 2022, “Simulation of a Safe Start-Up Maneuver for a Brayton Heat Pump,” *Proceedings of the ASME Turbo Expo 2022: Turbomachinery Technical Conference and Exposition*. *Volume 4: Cycle Innovations; Cycle Innovations: Energy Storage*. Rotterdam, Netherlands. V004T06A003. ASME. https://doi.org/10.1115/GT2022-79399.

[13] Pettinari, M., Frate, G. F., Tran, A. P., Oehler, J., Stathopoulos, P., and Ferrari, L., 2023, “Transient Analysis and Control of a Brayton Heat Pump during Start-Up,” *Proceedings of ECOS 2023: The 36th International Conference on Efficiency, Cost, Optimization, Simulation and Environmental Impact of Energy Systems*, Las Palmas de Gran Canaria, Spain, pp. 839–850. https://doi.org/10.52202/069564-0076.

[14] Oehler, J., Gollasch, J., Tran, A. P., and Nicke, E., 2021, “Part Load Capability of a High Temperature Heat Pump with Reversed Brayton Cycle,” *13th IEA Heat Pump Conference*, Jeju, Korea, p. 12.

[15] The MathWorks Inc., 2022, “MATLAB Version: 9.13.0 (R2022b),” https://www.mathworks.com (last accessed: 30/05/2023)

[16] Lemmon, E. W., Bell, I. H., Huber, M. L., and McLinden, M. O., 2018, “NIST Standard Reference Database 23: Reference Fluid Thermodynamic and Transport Properties-REFPROP, Version 10.0, National Institute of Standards and Technology.” https://doi.org/10.18434/T4/1502528.

[17] The MathWorks Inc., “Simscape Fluids Reference,”https://it.mathworks.com/help/pdf_doc/hydro/hydro_ref.pdf (last accessed: 30/05/2023).

[18] Holman, J. P., 2002, *Heat Transfer*, 9th ed., McGraw-Hill, New York, NY, ISBN: 978-0-07-352936-3.